

Modeling GPS multipath effect based on spherical cap harmonic analysis

Jin-yun GUO^{1,2}, Guo-wei LI^{1,2}, Qiao-li KONG^{1,2}, Shu-yang WANG^{1,2}

1. College of Geodesy and Geomatics, Shandong University of Science and Technology, Qingdao 266590, China;

2. Key Laboratory of Surveying and Mapping Technology on Island and Reef of NASMG, Qingdao 266590, China

Received 10 July 2013; accepted 13 January 2014

Abstract: Most GPS positioning errors can be eliminated or removed by the differential technique or the modeling method, but the multipath effect is a special kind of system or gross error, so it is difficult to be simulated or eliminated. In order to improve the accuracy of GPS positioning, the single-epoch pseudorange multipath effects at GPS station were calculated, and firstly modeled based on the spherical cap harmonic (SCH), which is the function of satellite longitude and latitude with the robust method. The accuracy of the kinematic point positioning technique was improved by correcting pseudorange observations with the multipath effect calculated by the SCH model, especially in the elevation direction. The spherical cap harmonic can be used to model the pseudorange multipath effect.

Key words: GPS; multipath effect; spherical cap harmonic; kinematic point positioning

1 Introduction

Multipath effect is one of major positioning error sources for navigation and positioning with GPS technique. Most GPS positioning errors, including the ionospheric delay error, tropospheric delay error, clock error and satellite orbital error, can be eliminated or removed by the differential technique or the modeling method [1]. But these methods are useless to eliminate the multipath effects [2]. So far, strategies to deal with the multipath effect can be classified as the hardware and software solutions [3]. The multipath effect is a special kind of system or gross error, so it is difficult to be simulated or eliminated [4].

When the environment surrounding the GPS station is steady, the multipath effect is related to the positions of the visible GPS satellites. To mitigate the multipath effect at permanent GPS stations, the multipath template technique was developed by taking advantage of the daily repetition of the GPS observations [5]. GE et al [6,7] ever mitigated the multipath effect by an adaptive filter based on the repeatability of the multipath and detected the multipath effect change for permanent GPS stations. KEE and PARKINSON [8] developed the dual

frequency method (DFM) and represented the pseudorange multipath effect by a linear combination of spherical harmonics, and other scholars modeled the multipath effects by other function forms [9,10]. HARRIS [11] evaluated and fused various methods to process the pseudorange multipath effect. RAY [12] investigated the multipath and developed a system for reducing the effect using multiple closely-spaced antennas. The multipath was parameterized using a Fourier analysis and a wavelet analysis technique [13]. The above researches are mostly carried on some special time windows or satellites. It is very difficult to isolate correctly the single-epoch multipath effect from all kinds of GPS positioning errors [14]. The calculation and model of the single-epoch multipath effect face with a lot of problems.

The spherical harmonic is widely used in modeling the multipath effect at permanent GPS stations, but this method costs a lot of computation resources and causes the ill-posed problems especially using the single-epoch data. To solve this problem, the spherical cap harmonic (SCH) is firstly adopted to model the pseudorange multipath effect in this work.

Firstly, the single-epoch pseudorange multipath effects at GPS stations were calculated. Then, trajectories

Foundation item: Project (41374009) supported by the National Natural Science Foundation of China; Projects (TJES1101, TJES1203) supported by the Key Laboratory of Advanced Engineering Surveying of NASMG, China; Project (ZR2013DM009) supported by the Shandong Natural Science Foundation of China; Project (201412001) supported by the Public Benefit Scientific Research Project of China

Corresponding author: Jin-yun GUO; E-mail: jinyunguo1@126.com

DOI: 10.1016/S1003-6326(14)63266-0

of GPS satellites were divided into three parts, and the multipath effects of different parts were modeled using the spherical cap harmonic (SCH). Finally, an experiment was designed to evaluate the effectiveness of the SCH model. Original pseudorange observation was corrected with the pseudorange multipath effect calculated by the model, and the kinematic coordinate of GPS station was estimated with the kinematic point positioning technique to test the effect of the model.

2 Pseudorange multipath effect

The multipath effect is a phenomenon of the delay of composite signal compared to the direct signal in the space constructed by the GPS satellite, the receiver antenna and the surrounding objects [4]. According to the basic principle of multipath effect, if the receiver is stationary and the surrounding objects don't change, the multipath effect repeats as the GPS constellation does. Theoretically, the pseudorange multipath effect is less than one code element width, while the phase multipath effect is no more than the quarter of one carrier-phase wavelength. The pseudorange multipath effect is usually computed using the linear combinations of the pseudorange and carrier phase data. The pseudorange multipath effects can be calculated as follows:

$$M_{P_1} = P_1 - (1 + \frac{2}{\alpha - 1})\varphi_1\lambda_1 + (\frac{2}{\alpha - 1})\varphi_2\lambda_2 =$$

$$M_1 - (1 + \frac{2}{\alpha - 1})n_1\lambda_1 + (\frac{2}{\alpha - 1})n_2\lambda_2 -$$

$$(1 + \frac{2}{\alpha - 1})m_1 + (\frac{2}{\alpha - 1})m_2 \quad (1)$$

$$M_{P_2} = P_2 - (\frac{2\alpha}{\alpha - 1})\varphi_1\lambda_1 + (\frac{2\alpha}{\alpha - 1} - 1)\varphi_2\lambda_2 =$$

$$M_2 - (\frac{2\alpha}{\alpha - 1})n_1\lambda_1 + (\frac{2\alpha}{\alpha - 1} - 1)n_2\lambda_2 -$$

$$(\frac{2\alpha}{\alpha - 1})m_1 + (\frac{2\alpha}{\alpha - 1} - 1)m_2 \quad (2)$$

where $\alpha = (f_1/f_2)^2$, f_1 and f_2 are the frequencies of L1 and L2 respectively; P_1 and P_2 are the pseudorange observations on L1 and L2; φ_1 and φ_2 are the carrier phase observations on L1 and L2; λ_1 and λ_2 represent the wavelengths of L1 and L2; n_1 and n_2 are the phase integer ambiguities of L1 and L2; M_1 and M_2 are the L1 and L2 pseudorange multipath effects mixed with noises; and m_1 and m_2 are the L1 and L2 phase multipath effects mixed with noises, respectively.

In the absence of cycle slips, the mean of the computed result of Eqs. (1) and (2) is removed to reduce the effect of the integer ambiguity. The carrier multipath effect and noise are smaller than the others in the residual.

The residual then contains the pseudorange multipath effect and receiver noise [12].

Taking DOY001 in 2007 of BJFS station as example, the pseudorange multipath effect is calculated using Eqs. (1) and (2), and plotted at each epoch with respect to the corresponding satellite azimuth and elevation angle at L1 and L2 with CF2SKY program [15], as shown in Figs. 1 and 2. The statistic of the pseudorange multipath effect in different regions of elevation is listed in Table 1. In Figs. 1 and 2, the elevation-cutoff angle is set to 10° , as shown in the grey area, the black curves are the trajectories of satellites, the red numbers are the PRN numbers of GPS satellites, and the green lines along the trajectories are the pseudorange multipath effects for each satellite. As listed in Table 1, when the elevation angle is below 30° , the pseudorange multipath effect is much larger. While the angle is above 30° , the multipath effect becomes smaller. The multipath effect above 60° is much small and steady, but it is also up to level of 10 cm which is not neglected in precise GPS navigation and positioning. Overall, the range of the multipath errors of BJFS is acceptable.

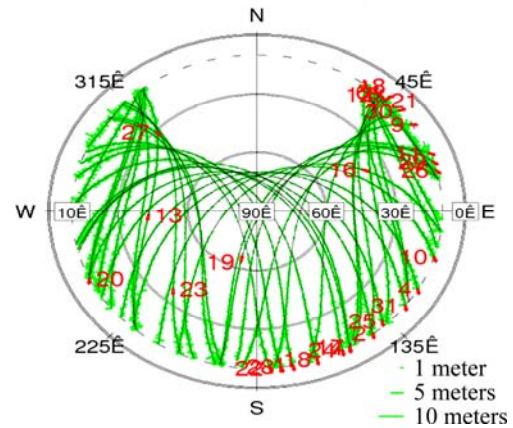


Fig. 1 Satellites distribution and P1 pseudorange multipath effect at station BJFS (DOY001, 2007)

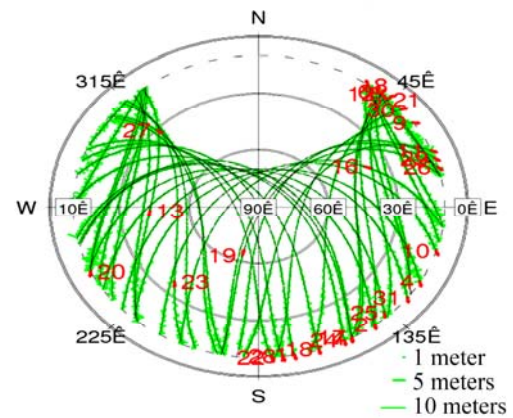


Fig. 2 P2 pseudorange multipath effect at station BJFS (DOY001, 2007)

Table 1 Statistic of pseudorange multipath effect in different regions of elevation

| Item | M_{P_1}/m | | | M_{P_2}/m | | |
|------|-------------|--------|--------|-------------|--------|--------|
| | 0–30 | 30–60 | 60–90 | 0–30 | 30–60 | 60–90 |
| Max | 5.035 | 1.578 | 0.368 | 3.967 | 1.205 | 0.349 |
| Min | −4.449 | −1.247 | −0.314 | −4.875 | −1.323 | −0.362 |
| Mean | 0.000 | −0.001 | 0.005 | −0.017 | 0.001 | −0.004 |
| STD | 0.738 | 0.248 | 0.097 | 0.734 | 0.256 | 0.098 |
| RMS | 0.738 | 0.248 | 0.097 | 0.735 | 0.256 | 0.098 |

3 Modeling pseudorange multipath effect using SCH

The spherical cap harmonic (SCH) is a spectral function based on the potential theory in the spherical cap coordinate system. The spherical coordinates $Q(r, \theta, \lambda)$ referred to the spherical coordinate system with the northern pole are denoted by $Q(r, \psi, l)$ in the spherical cap coordinate system with the new pole $P(\phi_c, L_c)$ (Fig. 3). When the coordinates of the points on the spherical cap are given in the ellipsoidal coordinate (ϕ, L) , the coordinate transformation has to be done to convert (ϕ, L) to (ψ, l) . The formulas for such transform are as follows:

$$\tan \phi = (1 - e^2) \cdot \tan \varphi \quad (3)$$

$$\theta = (\pi/2) - \phi \quad (4)$$

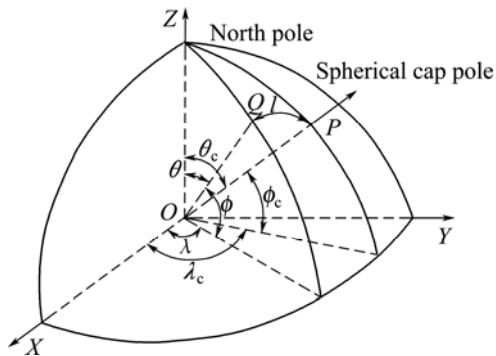
$$\lambda = L \quad (5)$$

So

$$\psi = \arccos(\cos \theta \cos \theta_c + \sin \theta \sin \theta_c \cos(\lambda_c - \lambda)) \quad (6)$$

$$l = \arctan\left(\frac{\sin \theta \sin(\lambda - \lambda_c)}{\cos \theta \sin \theta_c - \sin \theta \cos \theta_c \cos(\lambda_c - \lambda)}\right) \quad (7)$$

where ϕ is the geocentric latitude; (θ_c, λ_c) is converted from (ϕ_c, L_c) using Eqs. (3)–(5).

**Fig. 3** Coordinate transform from spherical coordinate system to spherical cap system

According to the spherical harmonic function used in modeling the multipath effect [8], the pseudorange

multipath effect expressed with SCH is expressed as

$$M_P = \sum_{k=-m}^{K_{\max}} \sum_{m=0}^k (\bar{C}_{km} \cos ml + \bar{S}_{km} \sin ml) \bar{P}_{n_k(m)}^m(\cos \psi) \quad (8)$$

where M_P is the multipath effect; ψ and l are the colatitude and longitude in the spherical cap coordinate system; $\bar{P}_{n_k(m)}^m(\cos \psi)$ is the normalized Legendre function with the non-integer degree; \bar{C}_{km} and \bar{S}_{km} are the coefficients of the SCH model; and $n_k(m)$ and m are the degree and order of the Legendre function respectively.

The $n_k(m)$ can be determined under the boundary condition [16]. Given $n_k(m)$ and m , the normalized Legendre function with the non-integer degree $\bar{P}_{n_k(m)}^m(\cos \psi)$ is as follows:

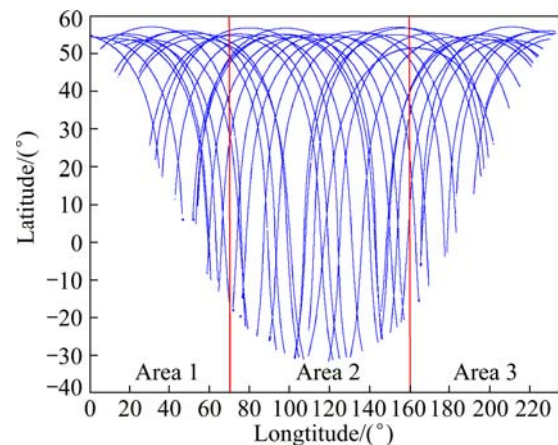
$$\bar{P}_{n_k(m)}^m(\cos \psi) = \sum_{j=0}^J A_j(m, n_k(m)) \sin^{2j}(\theta/2) \quad (9)$$

$$A_j(m, n) = \left[\frac{(j+m-1)(j+m)-n(n+1)}{j(j+m)} \right] A_{j-1}(m, n) \quad (10)$$

$$K_n^m = \begin{cases} 1, & m=0 \\ 2^{-m} \left(\frac{n+m}{n-m} \right)^{\frac{n}{2}} + \frac{1}{4} p^{\frac{m}{2}} \exp(e_1 + e_2), & m \neq 0 \end{cases} \quad (11)$$

where $p = (n/m)^2 - 1$; $e_1 = -(1/12m)(1-1/p)$; $e_2 = -(1/360m^3) \cdot (1+3/p^2+4/p^3)$.

If the receiver antenna is stationary and the surrounding objects don't change, the multipath effect changes only due to the positions of GPS satellites. The single-epoch longitude and latitude of visible satellites at station BJFS are calculated with the precise ephemeris of DOY002 in 2007, and the trajectory of the satellites is shown in Fig. 4. According to the distribution of the visible satellites, the trajectory is divided into three parts, each of which has its own spherical cap coordinate system determined by different poles and half angles.

**Fig. 4** Trajectory of visible satellites at station BJFS (DOY002, 2007)

The satellite longitudes and latitudes are converted to the colatitudes and longitudes in their own spherical cap coordinate systems using the above coordinate transform formulas. By large amounts of test data, the appropriate maximum degrees for three areas are decided. The poles, half angles and maximum degrees of different areas are listed in Table 2. The maximum degrees of different areas are so small that the model can reduce the amount of calculation, and it is difficult to cause the ill-posed problems.

Table 2 Pole, half angle and maximum degree of spherical cap in different area

| Area | Pole/(°) | Half angle/(°) | Maximum degree |
|------|-------------|----------------|----------------|
| 1 | (35.5, 20) | 37 | 12 |
| 2 | (115, 12.5) | 45 | 14 |
| 3 | (197, 20.5) | 37 | 12 |

The pseudorange multipath effect of each area is modeled by Eq. (8). Because Eqs. (1) and (2) may produce the gross error caused by the atmosphere in the low elevation, the coefficients \bar{C}_{km} and \bar{S}_{km} are calculated by the robust estimation using the iterative weight selection method [17] as

$$P_i = \begin{cases} P_i, & C_i \leq C_0 \\ P_i \times C_0 / C_i, & C_i > C_0 \end{cases} \quad (12)$$

where $C_i = |V_i|/\sigma_0$; V_i is the residual of the observation; σ_0 is the variance of unit weight; P_i indicates the weight of the observation; and C_0 is a constant. The modeling results are shown in Fig. 5.

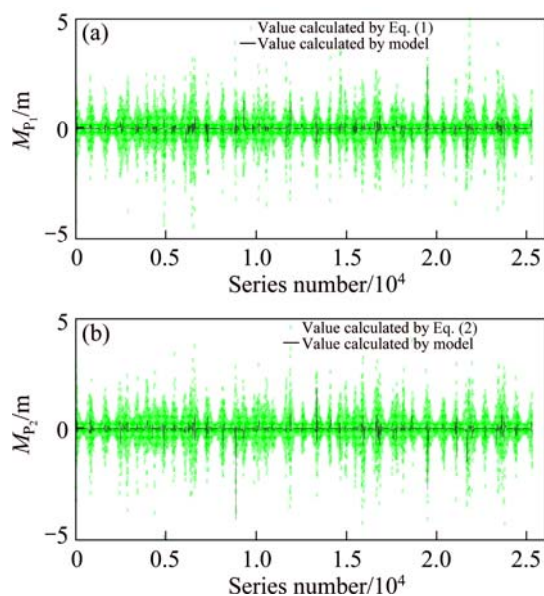


Fig. 5 P1 Pseudorange multipath effect calculated by SCH model and Eq. (1) (a); P2 Pseudorange multipath effect calculated by SCH model and Eq. (2) (b)

4 Analysis on kinematic point positioning

The pseudorange multipath effects for BJFS at DOY002 and DOY005, 2007, were modeled with the SCH method. P1 and P2 observations were corrected with the modeled pseudorange multipath effects, and then the kinematic coordinates of station BJFS was estimated using the kinematic point positioning portion of the Bernese GPS software [18], in which the precise ephemeris and high-rate satellite clocks (30 s) provided by CODE were used. Single-epoch coordinates were estimated using both the raw and corrected observations with the single-epoch point positioning technique [19]. The N, E, U displacements compared to the precise N, E, U coordinates were calculated, and the statistics of the displacements (d_N , d_E and d_U) of the two days were listed in Tables 3 and 4, respectively.

In Tables 3 and 4, the mean values of the displacements sequence are reduced after the correction of modeled multipath effect, especially in the elevation direction. On DOY002, the mean values reduced 7.6, 0.6, 86.3 cm in the N, E and U directions, respectively. Similarly, on DOY005, The mean values reduced 1.1, 2.0, 108.4 cm in the N, E and U directions, respectively. The mean of the displacements reflects the influence of the systematic error. So the improvement of mean is a result of the correction of the pseudorange multipath, which is one of the major systematic error sources of GPS technique. Because the modeled pseudorange multipath effect includes the noise components in Eqs. (1) and (2), the STD values do not improve as much as the mean value.

The improvement of RMS is mainly due to the improvement of the mean values. The RMS improvements in the N and E directions are small, but the improvements in the U direction are obvious, which are reduced by 11% and 18% on DOY002 and DOY005, respectively. The possible reasons of the phenomenon are as follows. Firstly, the environment surrounding BJFS is ideal, and there are no obvious reflected objects. It is well known that the multipath effect has a greater impact on positioning accuracy in U direction than that in N or E direction. So the improvement of multipath effect is not obvious in N and E directions. Secondly, the calculated results of Eqs. (1) and (2) are mixed with the receiver noises, and removing the ionospheric term actually increases the noise level [20], which leads to disorder especially in the low elevation. Meanwhile, the 30s sample rate data of all visible satellites are used. As a result, the maximum degree of SCH can't reach a high value to fit the change of the multipath effects calculated by Eqs. (1) and (2).

Table 3 Statistics of displacements of DOY002

| Condition | Direction | Displacement/m | | |
|-------------------|-----------|----------------|-------|-------|
| | | Mean | STD | RMS |
| Before correction | N | 0.689 | 0.862 | 1.104 |
| | E | 0.301 | 0.598 | 0.669 |
| | U | −0.928 | 1.813 | 2.037 |
| After correction | N | 0.613 | 0.857 | 1.054 |
| | E | 0.295 | 0.596 | 0.665 |
| | U | −0.065 | 1.812 | 1.813 |

Table 4 Statistics of displacements of DOY005

| Condition | Direction | Displacement/m | | |
|-------------------|-----------|----------------|-------|-------|
| | | Mean | STD | RMS |
| Before correction | N | 0.060 | 0.835 | 0.837 |
| | E | 0.037 | 0.576 | 0.577 |
| | U | −1.259 | 1.797 | 2.194 |
| After correction | N | 0.049 | 0.827 | 0.828 |
| | E | −0.017 | 0.576 | 0.576 |
| | U | −0.175 | 1.798 | 1.806 |

5 Conclusions

1) The spherical cap harmonic can be used to model the pseudorange multipath effect. This method costs little computation and avoids the ill-posed problems caused by the single-epoch data.

2) The results of BJFS station with the kinematic point positioning technique show the positioning accuracy especially in the elevation direction is improved by correcting pseudorange observations with the pseudorange multipath effect calculated by the SCH model.

3) The method can also improve the precision of GPS-RTK which will be used to monitor the subsidence in the coal mining [21]. What's more, some problems need to be investigated more deeply, such as how to divide the trajectory of the satellites to improve the degree of SCH.

References

- [1] GUO Jin-yun, XU Pan-lin, QU Guo-qing. Three-dimensional method for checking the antenna phase center bias of GPS receiver [J]. Geomatics and Information Science of Wuhan University, 2003, 28(4): 448–451 (in Chinese)
- [2] LI Zheng-hang, Huang Jin-song. GPS surveying and data processing [M]. Wuhan: Wuhan University Press, 2005. (in Chinese)
- [3] XIA L. Multipath in GPS navigation and positioning [J]. GPS Solutions, 2004, 8(1): 49–50.
- [4] XIA Lin-yuan. Theoretical research and numerical results regading multipath in GPS observation [D]. Wuhan: Wuhan University, 2001. (in Chinese)
- [5] BISSHOP G J, COCA D S, KAPPLER P H, HOLLAND E A. Studies and performance of a new technique for mitigation of pseudorange multipath effects in GPS ground stations [C]//Proceedings of the 1994 National Technical Meeting of The Institute of Navigation. San Diego, CA: The Institute of Navigation, 1994: 231–242.
- [6] GE L L, HAN S W, RIZOS C. Multipath mitigation of continuous GPS measurements using an adaptive filter [J]. GPS Solutions, 2000, 4(2): 19–30.
- [7] GE L L, HAN S W, RIZOS C. GPS multipath change detection in permanent GPS stations [J]. Survey Review, 2002, 36(283): 306–322.
- [8] KEE C, PARKINSON B W. Calibration of multipath errors on GPS pseudorange measurements [C]//Proceedings of the 7th International Technical Meeting of the Satellite Division of The Institute of Navigation. Salt Lake City, UT: The Institute of Navigation, 1994, 353–362.
- [9] WANNINGER L, MAY M. Carrier phase multipath calibration of GPS reference stations [J]. Navigation- Los Angeles and Washington-, 2001, 48(2): 113–124.
- [10] REICHERT A K, AXELRAD P. Carrier-phase multipath corrections for GPS-based satellite attitude determination [J]. Navigation Journal of the Institute of Navigation, 2001, 48: 77–88.
- [11] HARRIS R B. Evaluation, refinement and fusion of software-based pseudorange multipath mitigation techniques [C]//Proceedings of the 15th International Technical Meeting of the Satellite Division of The Institute of Navigation. Portland, OR: The Institute of Navigation, 2002, 460–471.
- [12] RAY J K. Mitigation of GPS code and carrier phase multipath effects using a multi-antenna system [D]. Canada: the University of Calgary, 2000.
- [13] EDWARD-MCGHEE K. Site-specific point positioning and GPS code multipath parameterization and prediction [D]. Ohio: the Ohio University, 2011.
- [14] BRAASCH M S. Isolation of GPS multipath and receiver tracking errors [J]. Navigation Journal of the Institute of Navigation, 1995, 41(4): 415–434.
- [15] HILLA S. Plotting pseudorange multipath with respect to satellite azimuth and elevation [J]. GPS Solutions, 2004, 8: 44–48.
- [16] HAINES G V. Compute programs for spherical cap harmonic analysis of potential and general fields [J]. Computers & Geoscience, 1988, 14(4): 413–447.
- [17] LIU Da-jie, TAO Ben-zao. Practical surveying data processing [M]. Beijing: Surveying and Mapping Press, 2003, 51–67. (in Chinese)
- [18] DACH R, HUGENTOBLE U, FRIDEZ P, MEINDL M. Bernese GPS software version 5.0 [M]. Berne, Switzerland: Astronomical Institute, University of Berne, 2007.
- [19] GUO J Y, YUAN Y D, KONG Q L, LI G W, WANG F J. Deformation caused by 2011 eastern Japan great earthquake monitored by GPS single-epoch precise point positioning technique [J]. Applied Geophysics, 2012, 9(4): 483–493.
- [20] GUO J Y, HAN Y B, CHANG X T. A new method of ionospheric-free hybrid differential positioning based on a double-antenna CAPS receiver [J]. Science in China Series G, 2009, 52(3): 368–375.
- [21] GAO J X, LIU C, WANG J, LI Z K, MENG X C. A new method for mining deformation monitoring with GPS-RTK [J]. Transactions of Nonferrous Metals Society of China, 2011, 21(S): s659–s664.

基于球冠谐分析的 GPS 多路径效应建模

郭金运^{1,2}, 李国伟^{1,2}, 孔巧丽^{1,2}, 王书阳^{1,2}

1. 山东科技大学测绘学院, 青岛 266590;

2. 海岛(礁)测绘技术国家测绘地理信息局重点实验室, 青岛 266590

摘 要: GPS 定位中的多数误差均可通过差分或模型的方式减弱或消除, 但多路径效应是一种比较特殊的系统误差, 不易被模拟或消除。为提高 GPS 定位精度, 计算 GPS 测站的单历元伪距多路径效应, 首次利用球冠谐分析 (SCH) 建立测站单历元伪距多路径效应与卫星经纬度之间的函数关系, 建模过程中采用抗差估计求解模型参数。在伪距观测数据中加入模型计算的伪距多路径效应改正, 伪距动态单点定位精度得到提高, 尤其是高程方向精度明显提高。球冠谐分析可用于建立伪距多路径效应模型。

关键词: GPS; 多路径效应; 球冠谐分析; 动态单点定位

(Edited by Chao WANG)